VISIBLE ABSORPTIONS OF POTENTIAL DIFFUSE ISM HYDROCARBONS: C_9H_9 AND C_9H_5 RADICALS

M. STEGLICH[1], S. MAITY[2], AND J. P. MAIER
Department of Chemistry, University of Basel, Klingelbergstrasse 80, 4056 Basel, Switzerland

ABSTRACT

The laboratory detection of previously unobserved resonance-stabilized C_9H_5 and C_9H_9 radicals in the supersonic expansion of a hydrocarbon discharge source is reported. The radicals are tentatively assigned as acetylenic-substituted cyclopentadienyl C_9H_5 and vinyl-substituted benzyl C_9H_9 species. They are found to feature visible absorption bands that coincide with a few very weak diffuse interstellar bands toward HD183143 and HD204827.

Key words: ISM: lines and bands – ISM: molecules – methods: laboratory: molecular – molecular data

1. INTRODUCTION

In the past two decades, the electronic spectra of a number of carbon chains and their ions could be obtained in the gas phase at low temperatures (Zack & Maier 2014, and references therein). The object of these studies was to be able to compare laboratory data with astronomical measurements of the diffuse interstellar bands (DIBs; e.g., Herbig 1995). The systems were relevant because radio astronomy has unambiguously identified polar carbon chains in dense clouds[3] and thus absorptions of those systems, which have their electronic transitions in the visible and near-infrared, were sought. The laboratory studies were successful for a number of bare carbon chains and their cations and anions, as well as those containing a few hydrogen atoms. It could be shown that none of their absorptions correspond to the known DIBs, which number up to 500 by now (Snow & McCall 2006). The general conclusion drawn was that such systems, comprising up to a dozen or so carbon atoms, cannot be responsible for the stronger DIBs. However, larger systems—like those with an odd number of at least fifteen carbon atoms—remain viable candidates, because they possess intense electronic transitions in the DIB range (Maier et al. 2004). Their spectra are known in the condensed phase (Forney et al. 1996; Wyss et al. 1999), but not yet in gas. Only recently, the fullerene cation C_{60}^+ was confirmed to carry five DIBs between 9349 and 9633 Å (Campbell et al. 2015, 2016; Walker et al. 2015).

Analysis of the apparent rotational profiles of a few DIBs with resolved structure has led Huang & Oka (2015) to conclude that their most likely carriers are smaller molecules with five to eight heavy atoms. The initially evident systems, such as C_6H and others, have already been studied, albeit with negative results (Motylewski et al. 2000). Therefore, we began to search for systems that have been omitted from our laboratory investigations until now. The first such example was the $H_2C_7H^+$ chain, the protonated form of the neutral cumulene, H_2C_7. The latter is a known constituent in dense clouds. Unfortunately, the absorption of $H_2C_7H^+$ falls in the region of a helium line, precluding a conclusion (Rice et al. 2015).

However, it could be argued that cations of smaller molecules in diffuse interstellar space are subject to electron recombination; hence, the neutral systems are of more relevance. In our studies of the electronic spectra of hydrocarbon radicals—also of interest as intermediates in combustion processes—we obtained spectra of a number of species of the type C_nH_m (e.g., Maity et al. 2015a, 2015b), i.e., carbonaceous molecules containing more than two or three hydrogens. Some of these fit into the category sought by Oka's work: a prolate structure and a small number of heavy atoms. In addition, hydrogenated carbonaceous matter is known to exist in the diffuse interstellar medium, as can be concluded from the ratio between the 3.4 and 3.3 μm absorptions (e.g., Steglich et al. 2013).

In this article, we report the electronic spectra of previously unobserved radicals with molecular formula C_9H_5 and C_9H_9 that seem to match a few weak DIBs found by Hobbs et al. (2008, 2009). The approach used to obtain the gas phase spectra was a multiphoton laser ionization technique applied on a molecular beam that contains the target species, under conditions found in diffuse interstellar clouds; i.e., with rotational temperatures of around 10 K.
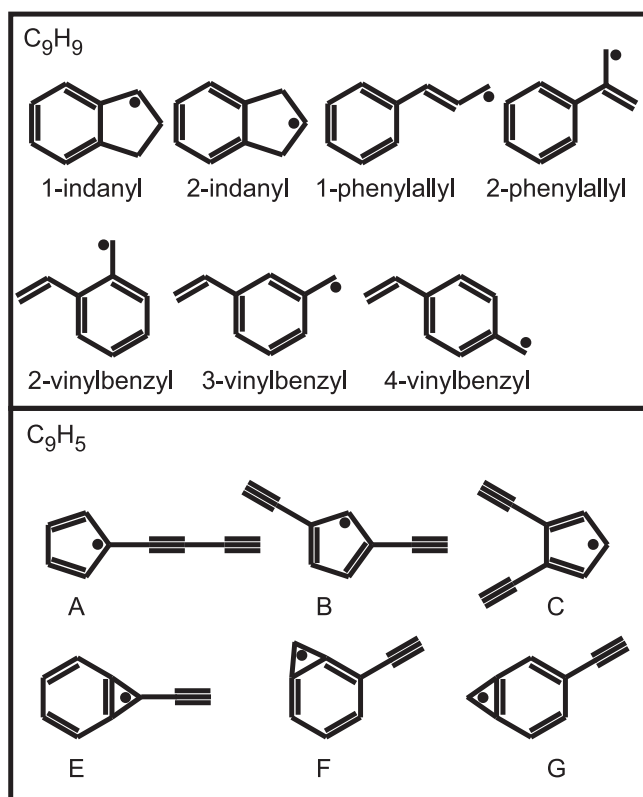
2. EXPERIMENT

Details of the experimental setup are discussed elsewhere (Maity et al. 2015a). The C_9H_9 and C_9H_5 radicals were produced, along with other molecules, in a pulsed electrical discharge of an organic precursor. The latter was a decomposition product of 0.1% 1,6-heptadiyne (C_7H_8) in He. The decomposition occurred during storage of the prepared gas bottle at 20 °C for at least 24 hr; a discharge of the freshly prepared gas mixture did not produce the target species. The molecular beam was created by skimming the supersonic expansion (5 bar backing pressure) at a distance of about 30 mm from the exit of the discharge source. Spectra in the 4200–7000 Å range were recorded using a resonant two-color two-photon ionization scheme. Photons with tunable energy, generated by an optical parametric oscillator (OPO; 20 Hz, ~5 ns, 0.5–3 mJ/pulse, bandwidth = 1 Å, λ uncertainty = 5 Å), or by a higher-resolution dye laser (20 Hz, ~5 ns, 0.5–2 mJ/pulse, $\Delta\lambda = 0.02$ Å), counterpropagate the molecular beam and excite electronic states upon resonance. Ionization is achieved 0–5 ns later by the fifth harmonic output (2128 Å, 1.5 mJ/pulse) of the same Nd:YAG laser that pumps the OPO or dye laser, respectively. Resulting ions were extracted into a

---

Figure 1. Structural formulae of the different radicals discussed in the text.

time-of-flight spectrometer and detected by a micro-channel plate.

The experiment is mass-selective, but several isomers are produced. The identification of the structures usually relies on comparison to quantum-chemical calculations of ionization energies, vibrational and electronic state energies, and vibrational progressions and rotational profiles. Those were obtained using density functional theory (DFT) and time-dependent DFT (TDDFT) as implemented in Gaussian09 (Frisch et al. 2013). The B3LYP functional (Becke 1988; Lee et al. 1988) was applied in conjunction with the cc-pVTZ basis set (Dunning 1989; Woon & Dunning 1993). Vibrational progressions and rotational profiles were simulated with Gaussian09 and PGOPHER (Western 2010).

## 3. RESULTS AND DISCUSSION

Resonance-stabilized hydrocarbon radicals (RSRs) are relatively long-lived species that can build up in high concentrations in energetic environments, such as plasmas, flames, planetary atmospheres, and interstellar space. Well-known examples include the allyl C_3H_5, propargyl C_3H_3, and benzyl C_7H_7 radicals, which are key components in benzene and soot formation in hydrocarbon combustion. The higher stability of these molecules, compared to other isomers, is caused by a delocalization of the unpaired electron. This effect can be even more pronounced in larger entities. Recent laser spectroscopic investigations report many such radicals in supersonic jets (Tsuge et al. 2006; Reilly et al. 2008, 2009a, 2009b; Troy et al. 2009, 2011, 2014; Sebree et al. 2010a, 2010b, 2011; Chalyavi et al. 2011, 2012; Kidwell et al. 2013, 2014; O'Connor et al. 2013, 2015; Maity et al. 2015a, 2015b). Several of them could be recognized among the discharge products of the (partly decomposed) 1, 6-heptadiyne precursor,

e.g., cis- and trans-1-vinylpropargyl C_5H_5 (Reilly et al. 2009b), 1, 4-pentadienyl C_5H_7 (Chalyavi et al. 2011), benzocyclopropenyl C_7H_5 (Maity et al. 2015b), benzyl C_7H_7 (Foster & Miller 1989), 1-phenylpropargyl C_9H_7 (Reilly et al. 2009a), and 1-indanyl C_9H_9 (Troy et al. 2009; Maity et al. 2015a). Furthermore, we observed the triplet chains HC_5H and HC_7H (Steglich et al. 2015; Ding et al. 2003), as well as previously unidentified species on masses corresponding to C_7H_5, C_7H_7, C_7H_9, C_8H_9, C_9H_5, and C_9H_9. The new C_9H_5 and C_9H_9 electronic absorptions, the strongest of which seem to agree with a few very weak DIBs, are presented in the following subsections. Structural formulae of C_9H_5 and C_9H_9 isomers are given in Figure 1.

3.1. C_9H_9

The most stable C_9H_9 isomer is the 1-indanyl radical. Its origin band at 4725 Å (Troy et al. 2009; Maity et al. 2015a) is the strongest feature in the $D_1 \leftarrow D_0$ progression. It was observed in this experiment, but about fifty times weaker than the most intense band of the new absorption system that is displayed in Figures 2 and 3 and summarized in Table 1. The next stable isomer is the 1-phenylallyl radical, with a ground state energy calculated 0.17 eV above 1-indanyl and a $D_1 \leftarrow D_0$ origin measured at 5206 Å (Sebree et al. 2011; Troy et al. 2011). This one was not detected here, albeit the photon energies of the used lasers would have allowed it. The ground state of the second indanyl radical, i.e., 2-indanyl, is calculated 0.45 eV higher than 1-indanyl. It should absorb more toward the blue around 3000 Å, outside of the scan range. The ground states of the 4-, 3-, and 2-vinylbenzyl radicals[4] (0.44 eV, 0.53, and 0.60 eV), and of the 2-phenylallyl radical (0.53 eV), are located at comparable energies. The $D_1 \leftarrow D_0$ transitions of the vinylbenzyl radicals are predicted to cause adiabatic absorptions between 2.20 and 2.40 eV, in proximity to the observed band system (1.97–2.23 eV). The 2-phenylallyl radical, on the other hand, should absorb somewhat further to the blue at 2.66 eV. By scanning the energy of the ionizing laser (using another OPO between 2200 and 2400 Å), the ionization energy (IE) of the 6288 Å band carrier was determined to be (7.3 ± 0.1) eV. The adiabatic IE of the 2-phenylallyl radical is calculated a bit too far toward the blue (7.71 eV) to justify a convincing assignment. The corresponding values of the vinylbenzyl radicals (6.81–7.07 eV), especially the meta one (7.07 eV), provide a slightly better match. The C_9H_9 isomers at the next higher ground state energies (0.72–0.91 eV above 1-indanyl) are aliphatic five- and six-membered carbon rings fused together, i.e., they have the same carbon skeleton as indanyl, but two hydrogens attached on one of the hexagon carbons, destroying their aromaticity. These structures also have predicted $D_1 \leftarrow D_0$ transitions close to the observed bands (2.04–2.40 eV adiabatic), but their calculated ionization energies are considerably lower (6.08–6.65 eV adiabatic). They can be excluded as potential carriers of the observed band system, leaving the three vinylbenzyl radicals and, possibly, the 2-phenylallyl radical as the most likely explanations. This assignment receives additional support in light of the detection of other monocyclic aromatics in the same experiment, especially the benzyl one.

---

[4] The configurational isomerisms of 2- and 3-vinylbenzyl will be neglected in the following discussion, which will treat only the trans isomers. The cis forms are calculated to be less stable by 0.02–0.07 eV. In the discharge experiments performed by Troy et al. (2011) and Sebree et al. (2011), only the more stable trans isomer of 1-phenylallyl could be detected.
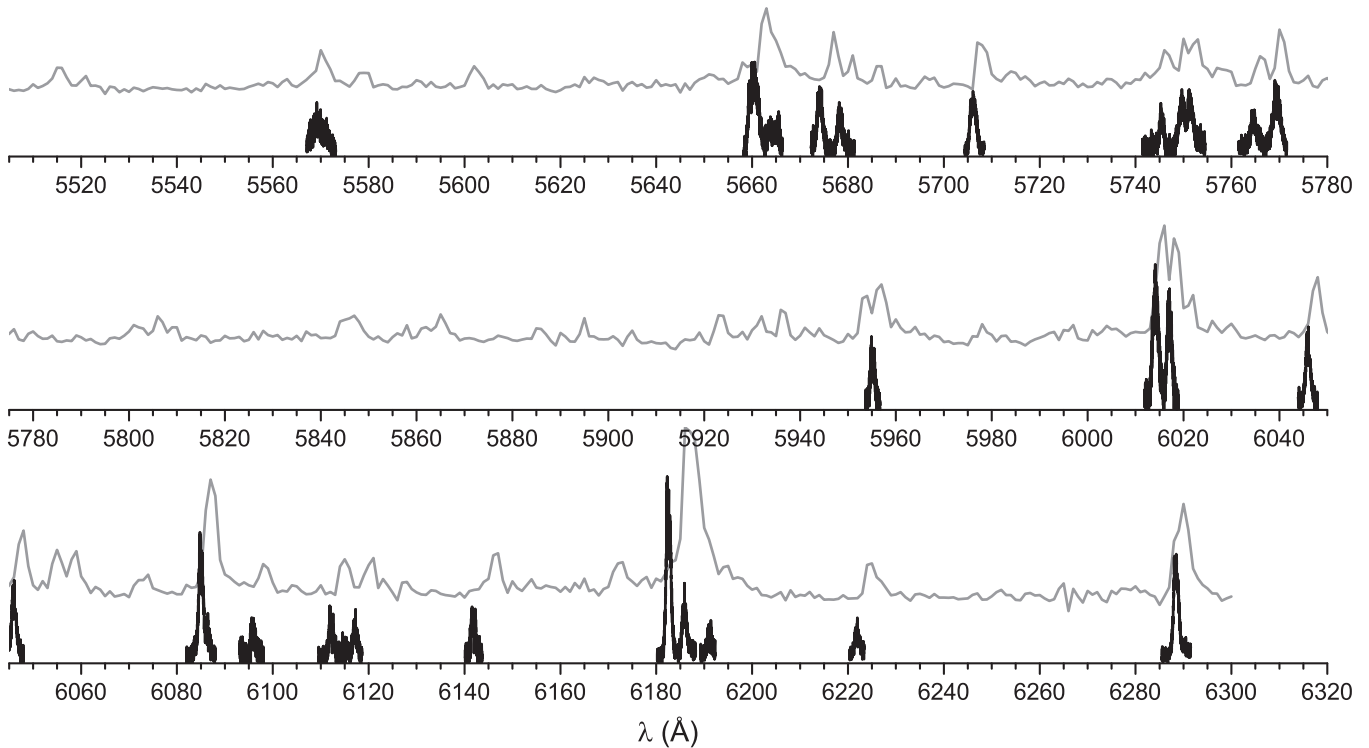
Figure 2. Absorption bands of C_9H_9 radicals. The OPO scan (1 Å bandwidth, 5 Å uncertainty) is displayed in gray and the higher-resolution scans (0.02 Å resolution) are the black traces.

The measured rotational profiles feature a Q branch centered between the P and R ones (see Figure 3). Assuming an asymmetric top rotor, this suggests a transition without a major geometry change that is of a-type, i.e., the dipole moment changes along the axis of smallest moment of inertia. This is in line with the suggested vinylbenzyl carriers, whose $D_1 \leftarrow D_0$ transitions are predicted to be mainly a-type. A simulation of the rotational contour of the para isomer, based on calculated geometries in $D_0(A'')$ and $D_1(A'')$ at $T_{rot} = 10$ K, is shown in the bottom panel of Figure 3. Apart from a somewhat stronger broadening of the bands at higher energies, the agreement between simulated and observed profiles is reasonable in terms of widths and positions of the branches. The meta- and ortho-vinylbenzyl isomers have similar profiles predicted. The simulated rotational profile of the $D_1(B) \leftarrow D_0(A)$ transition of 2-phenylallyl (not shown here) provides an equally good match, due to a mixed b and c character (about 1:1). A minor geometry change upon electronic transition should go along with a vibrational progression that is dominated by the origin band. Franck–Condon simulations indicate that this is true for the vinylbenzyl radicals rather than for 2-phenylallyl. Nevertheless, for such large molecules, the calculated vibrational frequencies in the excited state and Franck–Condon intensities are usually too unreliable for a confident assignment of the observed vibrational progression (assuming that several carriers contribute). The calculated adiabatic $D_1 \leftarrow D_0$ origin wavelengths and oscillator strengths are 5280 Å/$f = 2 \times 10^{-3}$ (para-vinylbenzyl), 5160 Å/ $f = 4 \times 10^{-4}$ (meta), and 5640 Å/$f = 1 \times 10^{-3}$ (ortho). Considering these values, the two strong bands at 6288 and 6183 Å may be assigned to the origin bands of ortho- and para-vinylbenzyl. Bands more toward the blue could belong to

vibronic excitations of all three vinylbenzyls and the 2-phenylallyl radical (4670 Å/$f = 3 \times 10^{-3}$). These features remain underdetermined until further experiments are performed, e.g., hole burning or use of specific precursors.

Table 2 compares the five strongest bands of the recorded C_9H_9 spectrum with tabulated DIB data from HD204827 and HD183143 (Hobbs et al. 2008, 2009). The positions of the laboratory bands at 6182 and 6085 Å are within 0.2 Å of two very weak DIBs (equivalent width $W < 10$ mÅ). Band widths (FWHM) of around 1 Å are similar in both cases. The relative intensities do not correlate as well. However, one has to keep in mind that the laboratory bands could stem from different isomers, and that extracting equivalent widths from such weak interstellar features comprises some uncertainties. Furthermore, the density of DIBs, especially weak ones, in this wavelength region is high. Unresolved overlaps are a possibility. This certainly seems to be a problem in the case of a strong ($W = 460...1880$ mÅ) DIB at 6284 Å, which is superposed by two to three weak features on its red shoulder that are near the 6288 Å laboratory band. Finally, very weak and narrow DIBs in HD204827 at 6019 and 6014 Å are comparable to the experimental bands at 6017 and 6014 Å. The same DIBs seem to appear in HD183143 around 6017 and 6015 Å, but were not tabulated.[5] A more detailed comparison of band shapes is hardly feasible because the signal-to-noise ratio of the astronomical data is too low.

How do the known electronic absorptions of the more stable C_9H_9 isomers compare with Hobbs et al.'s DIB data? The strongest band in the $D_1 \leftarrow D_0$ progression of 1-indanyl is the

---

[5] See full Figure 11 in Hobbs et al. (2008, 2009), available at http://dibdata.org.
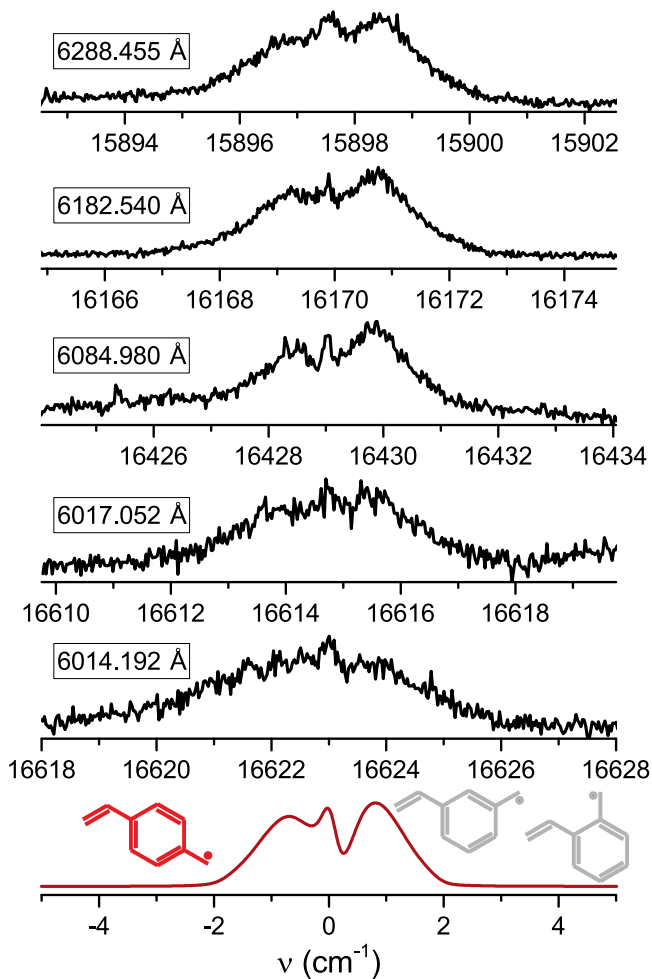
Figure 3. Higher-resolution observations of C_9H_9 absorptions. The bottom panel (red trace) is the calculated a-type rotational profile of 4-vinylbenzyl, based on optimized geometries in D_0 and D_1 ($T_{rot} = 10$ K). The meta and ortho isomers (3- and 2-vinylbenzyl; gray structures) have similar contours.

origin. It is at 4725 Å and has a width of 2 Å. A nearby DIB is at 4727 Å ($W = 284$ mÅ, FWHM $= 2.7$ Å in HD204827; $W = 156$ mÅ, FWHM $= 3.1$ Å in HD183143). Because of a 1 Å position mismatch, the 1-indanyl origin band was rejected as a possible carrier for the 4727 Å DIB (Troy et al. 2009). Considering the previously discussed coincidences of absorptions of other C_9H_9 isomers with DIBs that are about thirty times weaker than the 4727 Å one—and in light of comparable oscillator strengths of the $D_1 \leftarrow D_0$ transitions ($1 - 2 \times 10^{-3}$) —it could be argued that the 1-indanyl origin might be hidden beneath the strong DIB with which it was compared. The first transition of the trans-1-phenylallyl radical is also dominated by its origin, centered at 5205 Å. The calculated oscillator strength (1×10^{-3}) is about half that of the corresponding 1-indanyl transition. No DIBs are listed at 5205 Å, but a very weak interstellar feature—possibly matching the 1-phenylallyl absorption—seems to be present in the spectral data of HD204827.

3.2. C_9H_5

The absorption bands observed on $m/z = 113$, corresponding to C_9H_5, are plotted in Figures 4 and 5. Band positions, widths, and intensities are given in Table 3. The strongest band at 5719.46 Å (FWHM $= 0.99$ Å) matches a weak DIB in

Table 1
Absorption Bands of C_9H_9 Radicals

λ (Å)[a]	Intens.[b]	FWHM (Å)
6288.455	0.55	1.2
6221.946	0.21	1.36
6191.115	0.16	1.23
6185.875	0.3	1.12
6182.54	1	1.15
(6173)	0.17	…
6141.794	0.25	1.13
6117.138	0.22	1.01
6112.176	0.21	1.17
6095.904	0.18	1.19
6086.4	0.18	1.14
6084.98	0.66	1.09
(6074)	0.13	…
(6059)	0.25	…
(6055)	0.25	…
6045.968	0.35	1.17
(6022)	0.25	…
6017.052	0.58	1.23
6014.192	0.66	1.42
(5936)	0.19	…
(5932)	0.14	…
(5923)	0.17	…
(5895)	0.14	…
(5865)	0.16	…
(5847)	0.16	…
(5806)	0.15	…
5769.415	0.34	1.74
5764.688	0.19	1.61
(5757)	0.13	…
5751.415	0.29	1.36
5749.611	0.29	1.39
5745.425	0.23	0.95
5706.138	0.27	1.48
(5687)	0.13	…
5678.319	0.16	1.23
5674.143	0.28	1.29
(5668)	0.1	…
5660.386	0.45	2.55
(5660)	0.12	…
(5658)	0.13	…
(5602)	0.13	…
5571.262	0.1	0.83
5569.298	0.2	2.48
(5515)	0.13	…

Notes.
[a] Band center (higher-resolution scan with dye laser); accuracy of calibration is 0.02 Å. Values in brackets are uncalibrated OPO wavelengths (± 5 Å).
[b] Relative peak intensity; absolute error of ca. 0.05.

HD183143 (5719.63 Å; $W = 21.7$ mÅ; FWHM $= 0.92$ Å; Hobbs et al. 2009) and HD204827 (5719.48 Å; $W = 16.7$ mÅ; FWHM $= 0.69$ Å; Hobbs et al. 2008). The first band of the observed progression at 5904.39 Å (FWHM $= 1.17$ Å) is three times weaker than the strongest one. It also seems to coincide with a DIB at 5904.63 Å ($W = 4.6$ mÅ; FWHM $= 0.85$ Å) in HD204827. The same DIB appears in the spectrum of HD183143, but was not tabulated.

Several C_9H_5 isomers can be excluded as carriers of the experimental band system, due to differences between computed transition or ionization energies and measured values. Among these are all linear carbon geometries, which

<div align="center">

Table 2
Strongest C_9H_9 Absorptions, Compared to DIBs

</div>

| Laboratory			HD183143[a]			HD204827[b]		
λ^c (Å)	Intens.[d]	FWHM (Å)	λ (Å)	W (mÅ)	FWHM (Å)	λ (Å)	W (mÅ)	FWHM (Å)
6288.455	0.55	1.2	(6289.55)[e]	(19.2)	(1.63)	(6287.59)[e]	(13.9)	(0.51)
6182.54	1	1.15	6182.78	4.5	0.65	6182.58	6.4	1.04
6084.98	0.66	1.09	6085.09	8.9	1.29	6084.94	6.8	0.82
6017.052	0.58	1.23	?[f]	…	…	6019.32	4.2	0.79
6014.192	0.66	1.42	?[f]	…	…	6014.81	3.4	0.73

Notes.
[a] Hobbs et al. (2009).
[b] Hobbs et al. (2008).
[c] Band center; accuracy of calibration is 0.02 Å.
[d] Relative peak intensity; absolute error of ca. 0.05.
[e] Overlap with a strong DIB.
[f] Nearby weak DIBs appear in the spectrum, but are not tabulated.
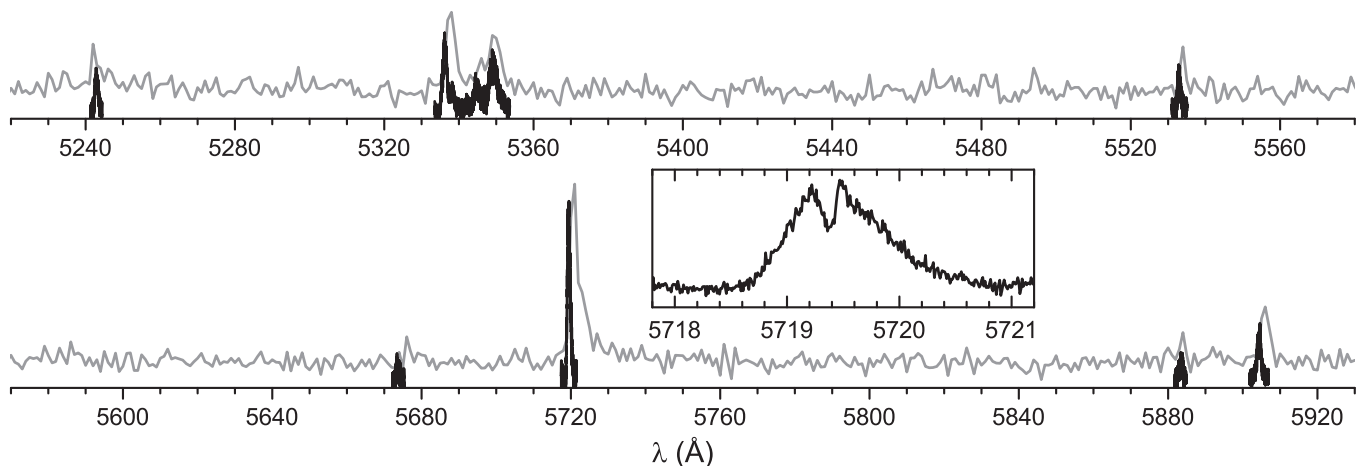
Figure 4. Absorption bands of C_9H_5 radicals. The OPO scan (1 Å bandwidth, 5 Å uncertainty) is displayed in gray; the higher-resolution scans (0.02 Å resolution) are shown as black traces. The inset is an expanded view of the strongest band.

are at least 1 eV above the ground state structure. In addition, the simulated rotational profiles of the chains are difficult to bring into agreement with the observed contours. All cyclic isomers—i.e., those forming one large carbon ring—either have no transitions predicted at the right energies, or are too far away from the ground state energy of the most stable isomer. Two classes of molecules remain as plausible candidates. The lower energy class is made of a cyclopentadienyl ring (C_5H_5), which has two acetylenic –C≡C– units attached, generating three different isomers. The molecule with the lowest ground-state energy is buta-1,3-diynyl-cyclopentadienyl H–C≡C–C≡C–(C_5H_4) (A). The other two are 1, 3- and 1, 2-diethynyl-cyclopentadienyl H–C≡C–(C_5H_3)–C≡C–H (B and C), which are slightly less stable by 0.16 and 0.25 eV, respectively. The computed vertical excitation energies of allowed transitions in C_9H_5-C are about 0.7 eV away from the observed absorptions, which were measured between 2.10 and 2.36 eV. Isomers A and B have much closer transitions, calculated at 2.57 and 2.71 eV (adiabatic energies) with

oscillator strengths $f = 0.07$ and $f = 0.1$, respectively. The simulated rotational contours in their $D_3 \leftarrow D_0$ transitions are compared to the measured profiles of the 5904 and 5719 Å bands in Figure 5, demonstrating a reasonable agreement. Weak Franck–Condon activities, with strong origin bands predicted for both isomers, are compatible with the absorption spectrum. The other class of possible carrier molecules is formed by attaching a single –C≡C– unit to benzocyclopropenyl C_7H_5, generating H-C≡C-(C_7H_4). This also gives three different isomers (E, F, G) that are less stable than A by 0.62–0.85 eV and have transitions predicted within 0.5 eV (adiabatic energy; $f = 4 \ldots 16 \times 10^{-3}$) of the observed system. Their simulated rotational profiles ($D_1 \leftarrow D_0$) are comparable to those of A and B, so they cannot be conclusively ruled out as possible band carriers.

4. SUMMARY

Visible absorption bands of previously unobserved C_9H_5 and C_9H_9 species were detected in the supersonic expansion of a
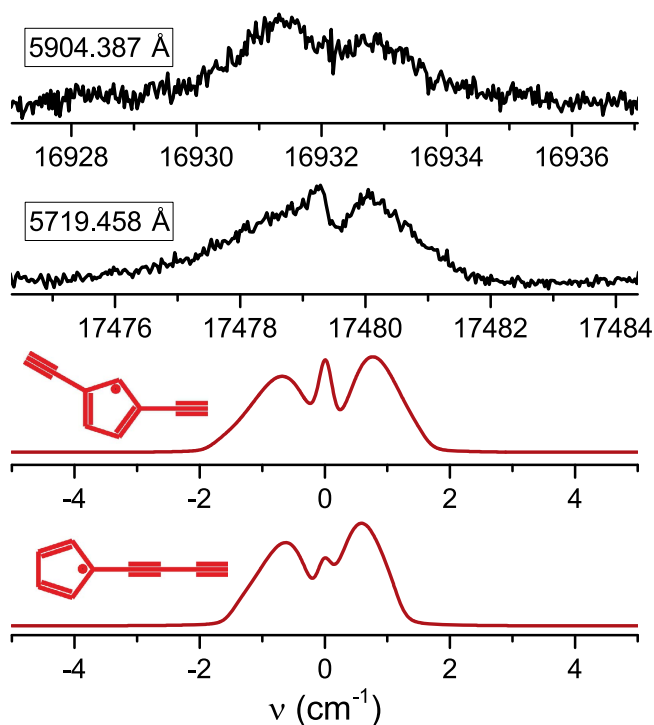
Figure 5. Higher-resolution observations of C_9H_5. The bottom panels (red traces) are $D_3 \leftarrow D_0$ rotational profile simulations of the lowest energy isomers ($T_{rot} = 10$ K).

Table 3
Absorption Bands of C_9H_5 Radical(s)

λ^a (Å)	Intens.[b]	FWHM (Å)
5904.387	0.31	1.17
5883.507	0.16	1.07
5719.458[c]	1	0.99
5673.589	0.14	1.02
5532.972	0.26	1.01
(5494)	0.14	…
5349.215	0.32	2.49
5344.861	0.19	1.73
5338.116	0.15	1.47
5336.225	0.45	1.28
(5297)	0.14	…
5242.934	0.27	0.96

Notes.
[a] Band center (higher-resolution scan with dye laser); accuracy of calibration is 0.02 Å. Values in brackets are uncalibrated OPO wavelengths (± 5 Å).
[b] Relative peak intensity; absolute error of ca. 0.05.
[c] The strongest band agrees with a weak DIB in HD183143 (5719.63 Å; $W = 21.7$ mÅ; FWHM $= 0.92$ Å) and HD204827 (5719.48 Å; $W = 16.7$ mÅ; FWHM $= 0.69$ Å).

hydrocarbon discharge source. The C_9H_5 radicals are tentatively assigned to resonance-stabilized buta-1, 3-diynyl-cyclopentadienyl H–C≡C–C≡C–(C_5H_4) and 1, 3-diethynyl-cyclopentadienyl H–C≡C–(C_5H_3)–C≡C–H. Isomers of vinyl-substituted benzyl probably carry the C_9H_9 absorptions. These assignments need to be verified in dedicated experiments, e.g., by applying carrier formation routes that use a more direct top-down approach (discharge of closely related precursors) or by probing the electronic ground state.

The strongest C_9H_9 bands are found to coincide with very weak DIBs toward HD183143 and HD204827. Assuming that the laboratory bands are due to vinyl-substituted benzyl isomers, the respective column densities are estimated between 1 and 3×10^{13} cm^{-2}, using $N = \frac{4\epsilon_0 m_e c^2 W}{e^2 \lambda^2 f}$. Two further weak DIBs seem to match laboratory bands of C_9H_5, which is supposed to be acetylenic substituted cyclopentadienyl. The corresponding column densities would be 0.5–1 $\times 10^{12}$ cm^{-2}. Unequivocal confirmation of the presence of C_9H_9 and C_9H_5 in diffuse interstellar space requires astronomical observations with higher signal-to-noise ratio.

REFERENCES

Becke, A. D. 1988, PhRvA, 38, 3098
Campbell, E. K., Holz, M., Gerlich, D., & Maier, J. P. 2015, Natur, 523, 322
Campbell, E. K., Holz, M., Maier, J. P., et al. 2016, ApJ, 822, 17
Chalyavi, N., Troy, T. P., Bacskay, G. B., et al. 2011, JChPh, 135, 124306
Chalyavi, N., Troy, T. P., Bacskay, G. B., et al. 2012, JPCA, 116, 10780
Ding, H., Schmidt, T. W., Pino, T., et al. 2003, JChPh, 119, 814
Dunning, T. H. 1989, JChPh, 90, 1007
Forney, D., Freivogel, P., Grutter, M., & Maier, J. P. 1996, JChPh, 104, 4954
Foster, S. C., & Miller, T. A. 1989, JPhCh, 93, 5986
Frisch, M. J., Trucks, G. W., Schlegel, H. B., et al. 2013, Gaussian 09, Revision D.01 (Wallingford, CT: Gaussian, Inc.)
Herbig, G. H. 1995, ARA&A, 33, 19
Hobbs, L. M., York, D. G., Snow, T. P., et al. 2008, ApJ, 680, 1256
Hobbs, L. M., York, D. G., Thorburn, J. A., et al. 2009, ApJ, 705, 32
Huang, J., & Oka, T. 2015, MolPh, 113, 2159
Kidwell, N. M., Mehta-Hurt, D. N., Korn, J. A., Sibert, E. L., & Zwier, T. S. 2014, JChPh, 140, 214302
Kidwell, N. M., Reilly, N. J., Nebgen, B., et al. 2013, JPCA, 117, 13465
Lee, C., Yang, W., & Parr, R. G. 1988, PhRvB, 37, 785
Maier, J. P., Walker, G. A. H., & Bohlender, D. A. 2004, ApJ, 602, 286
Maity, S., Steglich, M., & Maier, J. P. 2015a, JPCA, 119, 9078
Maity, S., Steglich, M., & Maier, J. P. 2015b, JPCA, 119, 10849
Motylewski, T., Linnartz, H., Vaizert, O., et al. 2000, ApJ, 531, 312
O'Connor, G. D., Bacskay, G. B., Woodhouse, G. V. G., et al. 2013, JPCA, 117, 13899
O'Connor, G. D., Woodhouse, G. V. G., Troy, T. P., & Schmidt, T. W. 2015, MolPh, 113, 2138
Reilly, N. J., Kokkin, D. L., Nakajima, M., et al. 2008, JAChS, 130, 3137
Reilly, N. J., Nakajima, M., Gibson, B. A., Schmidt, T. W., & Kable, S. H. 2009, JChPh, 130, 144313
Reilly, N. J., Nakajima, M., Troy, T. P., et al. 2009, JAChS, 131, 13423
Rice, C. A., Hardy, F.-X., Gause, O., & Maier, J. P. 2015, ApJL, 812, L4
Sebree, J. A., Kidwell, N. M., Buchanan, E. G., Zgierski, M. Z., & Zwier, T. S. 2011, Chem. Sci., 2, 1746
Sebree, J. A., Kislov, V. V., Mebel, A. M., & Zwier, T. S. 2010a, FaDi, 147, 231
Sebree, J. A., Kislov, V. V., Mebel, A. M., & Zwier, T. S. 2010b, JPCA, 114, 6255
Snow, T. P., & McCall, B. J. 2006, ARA&A, 44, 367
Steglich, M., Fulara, J., Maity, S., Nagy, A., & Maier, J. P. 2015, JChPh, 142, 244311
Steglich, M., Jäger, C., Huisken, F., et al. 2013, ApJS, 208, 26
Troy, T. P., Chalyavi, N., Menon, A. S., et al. 2011, Chem. Sci., 2, 1755
Troy, T. P., Nakajima, M., Chalyavi, N., et al. 2009, JPCA, 113, 10279
Troy, T. P., Tayebjee, M. J. Y., Nauta, K., Kable, S. H., & Schmidt, T. W. 2014, CPL, 620, 129
Tsuge, M., Hamatani, S., Kawai, A., Tsuji, K., & Shibuya, K. 2006, PCCP, 8, 256
Walker, G. A. H., Bohlender, D. A., Maier, J. P., & Campbell, E. K. 2015, ApJL, 812, L8
Western, C. M. 2010, PGOPHER, version 7.1.108 (Univ. Bristol), http://pgopher.chm.bris.ac.uk
Woon, D. E., & Dunning, T. H. 1993, JChPh, 98, 1358
Wyss, M., Grutter, M., & Maier, J. P. 1999, CPL, 304, 35
Zack, L., & Maier, J. P. 2014, Chem. Soc. Rev., 43, 4602